Selective sorption of rubidium by potassium cobalt hexacyanoferrate

Gayathri Naidu, Tanjina Nur, Paripurnanda Loganathan, Jaya Kandasamy, Saravanamuthu Vigneswaran*

Faculty of Engineering, University of Technology Sydney (UTS), P.O. Box 123, Broadway, NSW 2007 Australia,

*Corresponding author: Tel +61-2-9514-2641; Fax +61-2-9514-2633; Email: Saravanamuth.Vigneswaran@uts.edu.au

Abstract

Recovering economically valuable rubidium (Rb) from natural resources is challenged due to its low concentration and limited selectivity of extracting agents. Equilibrium and kinetic studies were conducted on the sorptive removal of Rb at low concentration (5 mg/L) using a commercial and a laboratory prepared potassium cobalt hexacyanoferrate (KCoFC). These laboratory and commercial KCoFCs exhibited similar characteristics in terms of chemical composition, surface morphology (scanning electron microscopy) and crystal structure (X-ray diffraction peaks). KCoFC exhibited a higher sorption capacity for Rb (Langmuir maximum sorption 96.2 mg/g) and cesium (Cs) (Langmuir maximum sorption 60.6 mg/g) compared to other metals such as lithium (Li), sodium (Na) and calcium (Ca) (sorption capacity < 2 mg/g). KCoFC sorption capacity for Rb was affected only when Cs was present at twice the concentration of Rb, while the influence of other metals (Li, Na, and Ca) was minimal even at high concentrations. High Rb sorption capacity was due to the exchange of Rb for K inside the crystal lattice and strong sorption on the sorbent surface. These were evident from the data on K release during Rb sorption and reduced negative zeta potential at the sorbent surface in the

presence of Rb, respectively. Kinetic sorption of Rb was satisfactorily described by the pseudo-second order model with intraparticle diffusion and exchange of Rb with structural K acting as major rate limiting steps. Up to 80% desorption of Rb was achieved with 0.1 M KCl. Overall, the results established the superior selectivity of KCoFC for Rb sorption.

Keywords: *potassium cobalt hexacyanoferrate; rubidium; sorption isotherm; sorption kinetics*

Highlights

- Potassium cobalt hexacyanoferrate (KCoFC) had high sorption capacity for Rb
- Rb was selectively sorbed by KCoFC in the presence of other alkali metals
- Langmuir sorption capacity was higher for Rb than Cs
- K release from KCoFC lattice was highest for Rb sorption among the alkali metals
- Intra-particle diffusion and lattice K release controlled Rb sorption kinetics

1. Introduction

In the last few decades attention has been focused on extracting rubidium (Rb) due to its application in many fields of science and technology. Rb is used in fibre optic telecommunication systems, semiconductor technology and night-vision equipment [1,2]. In recent years, new and more efficient techniques have been established in optical and laser application with the usage of warm Rb vapour [3,4]. Although considerable Rb mineral resources are available, it is much more difficult to extract Rb than other alkali metals [2]. The application potential coupled with the mineral extraction challenge has increased the economic value of Rb. The price of Rb is much higher (€7856.64/kg) in comparison to lithium (Li) (€1.22/kg) and potassium (K) (€0.11/kg) [5].

This has led to the development of new methods for the extraction of Rb from resources such as oilfield water, mining industry, ores with low Rb content, seawater and salt lakes [2,6-8]. Potential methods of alkali metal extraction from natural resources include evaporation,

precipitation, use of emulsion membranes and liquid–liquid extraction techniques [9,10]. Nevertheless, the effectiveness of recovering trace metals with these methods are challenged in natural resources by the low concentration of the target metals, the limited selectivity of the extracting agents, and the presence of other constituents. In this regard, inorganic ion-exchange sorbents offer a practical approach in that they have the capacity to selectively extract low concentration metals from mixed solutions [7].

A number of diverse inorganic sorbents have been used for selective alkali metal sorption including Prussian blue [11], potassium metal hexacyanoferrate [12], zeolite [13], titanium dioxide [14] and ammonium molybdophosphate [15]. Most of these studies have focused on the removal of radioactive cesium (Cs) in nuclear waste brine. Cs and Rb have similar physico-chemical properties and on this basis, a few studies have examined the prospect of Rb extraction by sorbents [5,16]. These studies have highlighted the high Rb sorption capacity of potassium metal hexacyanoferrate. However, we still lack a detailed understanding of: firstly, the mechanism and kinetics of Rb sorption by potassium metal hexacyanoferrate; and secondly, the effect of the presence of other alkali metals on Rb sorption. Moreover, these studies were conducted using high concentrations of the target alkali metal in the 20 to >500 mg/L range. The concentration of the target metal is an important factor in establishing the effective performance of a sorbent. As Rb is present in a relatively low concentration (<1.0 mg/L) in natural resources such as seawater, experiments at high concentration levels may not reflect the performance of the sorbent in a practical scenario. Further, apart from the sorption performance, desorption capacity is an important factor in establishing the viability of a sorbent if the target metal has to be recovered in concentrated form in solutions. This aspect has not been discussed thus far for Rb sorption with potassium metal hexacyanoferrate.

Hence, the objective of this study was to establish the selective affinity of potassium cobalt hexacyanoferrate (KCoFC) for Rb sorption. The specific objectives were to: (1) synthesise KCoFC in the laboratory (KCoFC(L)) and compare its properties and characteristics

with a commercial KCoFC sorbent (KCoFC(C)) in terms of chemical composition, crystal structure, surface area and pore size distribution, surface charge characteristics, and efficiency of Rb sorption; (2) determine the effect of pH and co-existing alkali metal ions on Rb sorption; (3) model the equilibrium and kinetics of Rb sorption; (4) determine the mechanism of Rb sorption; and (5) investigate the desorption of Rb using different acid, alkaline, and salt solutions.

2. Material and methods

2.1. Materials

2.1.1. Commercial sorbent (KCoFC(C))

KCoFC(C) also known as CsTreat was supplied by Fortum Engineering Ltd, (Finland). This sorbent consisted of dark brown-black granules ranging in size from 0.25 to 0.85 mm [17]. The granules were ground to particle sizes of 0.25 to 0.45 mm for this study.

2.1.2. Laboratory sorbent (KCoFC(L))

KCoFC(L) was prepared in the laboratory by adding 1 volume of 0.5 M potassium ferrocyanide trihydrate ($K_4Fe(CN)_6 \cdot 3H_2O$) to 2.4 volumes of 0.3 M cobalt nitrate hexahydrate ($Co(NO_3)_2 \cdot 6H_2O$) as described by Prout et al. [18]. The mixture was stirred for 1 h at room temperature, followed by centrifuging and washing with deionised water. The concentrated mixture was dried at 115^{o}C for 24 h. The dried granules were ground to a particle size of 0.25 to 0.45 mm, washed again with deionised water and then dried.

2.1.3. Solutions

Stock solutions of Rb, Cs, Li, K, Na and Ca were prepared by dissolving RbCl, CsCl, LiCl, KCl, NaCl and $CaCl_2$, respectively, in deionised water. All reagents were of analytical grade (Sigma-Aldrich) and were used without further purification.

2.2. Sorbent characterisation

2.2.1. Chemical analysis

Samples of KCoFC (0.05 g) were decomposed in 1 mL of concentrated H_2SO_4 by heating at 200°C for 5 h. 10 mL of 0.1 M H_2SO_4 was added to the residue, and diluted to 50 mL with deionised water as per the procedure of Nilchi et al. [19]. Concentrations of K, iron (Fe) and cobalt (Co) in the aqueous samples were measured after filtration through a 1.2 µm syringe membrane filter using Microwave Plasma - Atomic Emission Spectroscopy (MP-AES) (Agilent 4100). The procedure was carried out in triplicate and the average results are reported in this study. The deviation between the replicated values was < 10%.

2.2.2. SEM-EDX analysis

The morphology and detection of elements on the KCoFC before and after Rb sorption was carried out with scanning electron microscopy (SEM) coupled with Energy Dispersive X-ray spectrometry (EDX) operated at 15 kV (Zeiss Supra 55VP Field Emission).

2.2.3. Powder X-ray diffraction analysis (XRD)

XRD data (on powders) were collected on a Siemens D5000 diffractometer operating with CuKa radiation and a rotating sample stage. The samples were scanned at room temperature in the 2Θ angular range of 20–110°.

2.2.4. Surface area and pore volume

Nitrogen adsorption-desorption on KCoFC(C) and KCoFC(L) was determined at 77 K using the nano POROSITY (Mirae SI, Korea) adsorption analyser. Approximately 0.1 g of freeze-dried sample was used for the analysis following an overnight degassing at 80^0C under vacuum. The specific surface area was calculated using the standard Brunauer–Emmett–Teller

(BET) method. The total pore volume (V_{tot}) was determined from the nitrogen adsorption at a relative pressure of about $p/p_0 \approx 0.99$. Average pore diameter was calculated using the equation, $4V_{tot}/ S_{BET}$.

2.2.5. pH and zeta potential

To investigate the effect of pH and zeta potential on sorption, suspensions of 1 g/L KCoFC sorbents in different solutions (100 mL) were agitated for 12 h in a flat shaker at a shaking speed of 120 rpm at room temperature (24 ± 1ºC). The pH values of the feed solution were set in the 3 to 10 range by adjusting the initial pH using 0.1 M HCl and 0.1 M NaOH. The initial and final pHs at the end of the sorption period were measured using a HQ40d portable pH Meter. To maintain a constant pH, pH was adjusted to its initial value after 4 and 8 h for all sorption experiments. The zeta potential was measured using a Zetasizer nano instrument (Nano ZS Zen3600, Malvern, UK) on the suspensions. Measurements were done in triplicate to minimise undesirable biases (with differences between replicates always being less than 5%).

2.3. Sorption experiments

In view of the low concentrations of Rb and Cs in natural resources, and in order to reliably measure the metals concentrations utilising analytical instruments, sorption experiments were carried out at a maximum initial concentration of 5 mg/L for Rb and Cs. However, higher concentrations of Li, Na, and Ca were used as these metals had very low sorption capacity at low concentrations. All experiments were performed in a set of glass flasks containing 100 mL of metal solutions and different doses of sorbents agitated in a flat shaker at a shaking speed of 120 rpm at room temperature (24 ± 1ºC). The experiments were duplicated and the average values were recorded for data analysis. The difference between duplicate values was within ±2%. The concentrations of Rb, Li, Na and Ca in the supernatants were measured

using MP-AES. The Cs concentration was measured using ICS-MS (PerkinElmer® NexION® 300).

2.3.1. Sorption isotherms

Equilibrium sorption experiments were conducted with different doses of sorbent (KCoFC) ranging from 0.02 to 0.20 g/L at pH 7.0 ± 0.5. The suspensions were agitated for 24 h to reach the sorption equilibrium. The supernatant solution was examined using MP-AES analysis after filtration through a 1.2 µm syringe membrane filter. The sorption amount at equilibrium, q_e (mg/g), was calculated using Eq. (1):

$$q_e = \frac{(C_0 - C_e).V}{M} \quad (1)$$

where, C_0 and C_e are the initial and equilibrium concentration of ion in the bulk solution (mg/L), V is volume of solution (L) and M is mass of sorbent (g).

The sorption data were modelled according to Langmuir (Eq. 2) and Freundlich isotherms (Eq. 3) as follows.

$$q_e = \frac{Q_{max} K_L C_e}{1 + K_L C_e} \quad (2)$$

$$q_e = K_f C_e^{1/n} \quad (3)$$

$$q_e = K_f C_e^{1/n}$$

where Q_{max} is the maximum sorption capacity (mg/g), K_L is the Langmuir binding constant, which is related to the energy of sorption (L/mg), K_f is the Freundlich constant representing the

sorption capacity (mg/g)(L/mg)$^{1/n}$ and 1/n is a constant inversely related to the sorptive energy between the sorbent and the sorbate (unit-less).

2.3.2. Sorption kinetics

Sorption kinetics experiments for Rb and Cs were conducted by agitating KCoFC at a dose of 0.05 g/L with 5 mg/L of Rb and Cs in 0.1 L solution. Samples of the agitated suspensions were taken at different time intervals up to 48 h, filtered, and the filtrate analysed for Rb and Cs. The sorption amount (q_t) at time t was calculated using Eq. (4):

$$q_t = \frac{(C_0 - C_t).V}{M} \tag{4}$$

where, C_0 and C_t are the initial and final concentrations of metal at time t (mg/L).

The sorption data was modelled using pseudo-first order (PFO) and pseudo-second order kinetics (PSO) as described in (Eq. 5) and (Eq. 6) [20].

$$\ln(q_e - q_t) = \ln q_e - k_1 t \tag{5}$$

$$\frac{t}{q_t} = \frac{1}{k_2 q_e^2} + \frac{1}{q_e} t \tag{6}$$

where q_t (mg/g) is the adsorption capacity at time t (min), and k_1 (1/min) and k_2 (g/mg min) are the pseudo-first order and pseudo-second order rate constants, respectively.

The Weber-Morris diffusion model (Eq. 7) was also used to describe the kinetic data [21]:

$$q_t = k_i t^{1/2} + C \tag{7}$$

where k_i (mg/g min$^{0.5}$) is the intra-particle diffusion rate constant and the intercept C represents the boundary layer thickness.

2.4. Desorption

Initially Rb was sorbed onto KCoFC by shaking 0.1 g/L dose of the sorbent with Rb at a concentration of 5 mg/L. Upon saturation of the sorbent with Rb, the sorbent was filtered and dried at room temperature. The amount of Rb sorbed was determined as explained previously. The Rb in the sorbent was then desorbed using 0.1 M of HNO_3, KOH, KCl, NaCl, HCl, or NaOH. Desorption was carried out by shaking the Rb-saturated KCoFC with 50 mL of the reagents in a flat shaker at a shaking speed of 120 rpm for 30 min. The desorbed solutions were analysed for Rb concentration with MP-AES.

3. Results and discussion

3.1. Characteristics of KCoFC

3.1.1. Chemical decomposition analysis

The chemical decomposition analysis showed that both KCoFC(L) and KCoFC(C) had reasonably similar chemical composition (**Table 1**). For KCoFC(L), the K/Fe atomic ratio was 2.4 and Co/Fe atomic ratio was 1.6, while the corresponding ratios were 2.3 and 1.8, for KCoFC(C). Previous studies have reported a similar composition for hexacyanoferrate sorbents [19,22]. For instance, Mardan et al. [22] found the stoichiometric composition of a potassium cobalt hexacyanoferrate to be $K_{2.42}Co_{1.74}Fe(CN)_6$.

Table 1. Chemical composition of KCoFC

		Before Rb sorption			After Rb sorption		
		K	Fe	Co	K	Fe	Co
KCoFC(L)	mg/g	127.8 ± 3.1	77.1 ± 4.1	130.3 ± 2.3	69.3 ± 2.7	71.3 ± 3.2	114.4 ± 5.4
	wt%	12.8	7.7	13.0	6.9	7.1	11.4
	mmol/g	3.3	1.4	2.2	1.8	1.4	1.9
KCoFC(C)	mg/g	137.4 ± 2.3	85.8 ± 3.1	157.7 ± 0.9	69.6 ± 3.7	83.3 ± 2.3	128.7 ± 1.5
	wt%	13.7	8.6	15.8	7.0	8.3	12.9
	mmol/g	3.5	1.5	2.7	1.8	1.5	2.2

3.1.2. SEM-EDX analysis

The SEM images showed that KCoFC(L) and KCoFC(C) had a similar appearance, i.e. a porous and rough morphology before Rb sorption (**Fig. 1a**). After Rb sorption, no significant morphological changes were observed on the KCoFC sorbents (**Fig. 1b**).

The EDX emission pattern revealed the presence of K, Fe, and Co peaks in the samples representing the main metals of the KCoFC. The semi-qualitative element analysis showed that for KCoFC(L), the atomic ratio for K/Fe was 1.2 while for Co/Fe it was 1.4. Similarly, for KCoFC(C), the corresponding ratios were 1.0 and 1.5, respectively. Both the EDX and chemical decomposition analysis indicated a good match for the atomic ratio of Co/Fe (1.4 and 1.5 for EDX vs 1.6 and 1.8 for chemical decomposition). On the other hand, the K/Fe ratio for the EDX analysis was much lower (K/Fe 1.0-1.2) compared to the chemical decomposition analysis (K/Fe 2.4). This could be due to the limitation of EDX emission in capturing K that is located in the body/centre of the cubic caged KCoFC structure, in comparison to Fe and Co which are primarily located at the corners of the structure [23]. The low K/Fe atomic ratio of 1.0-1.2

obtained was consistent with a recent study reporting a K/Fe atomic ratio of 1.23 for potassium nickel hexacyanoferrate using EDX analysis [24].

Upon Rb sorption, a peak of Rb in the energy zone of 1.7 keV was observed in the EDX spectra with a reduction of K peak intensity, suggesting the sorption of Rb with the exchange of K (**Fig. 1b**). Consistent with this, for both KCoFC(C) and KCoFC(L) a slight reduction in K/Fe ratio was detected following Rb sorption while no difference was observed for the Co/Fe ratio. The chemical composition analysis (**Table 1)** was able to show a clear reduction of K/Fe ratio upon Rb sorption from 2.3 - 2.4 to 1.2 -1.3 with minimal change of Co/Fe.

(a)

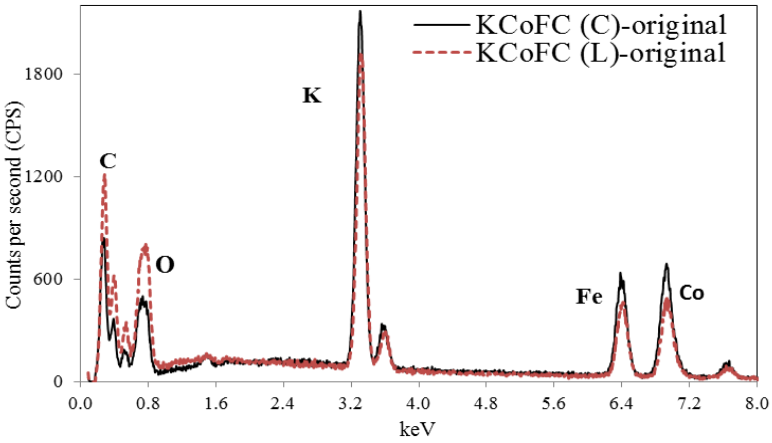

KCoFC(L)	% atomic ratio
K/Fe	1.2
Co/Fe	1.4

KCoFC(C)	% atomic ratio
K/Fe	1.0
Co/Fe	1.5

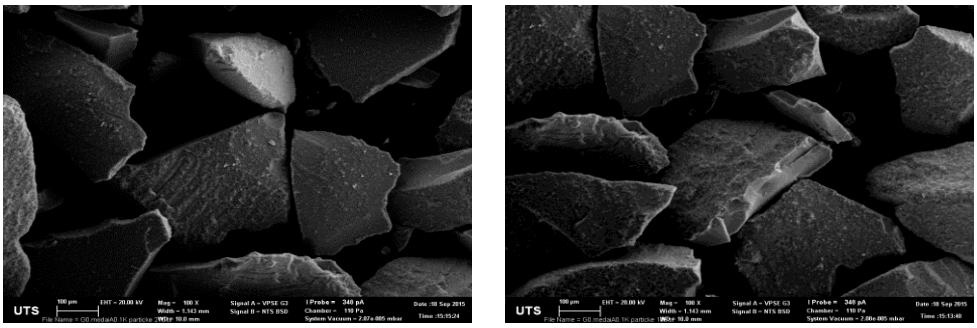

KCoFC(C) **KCoFC(L)**

(b)

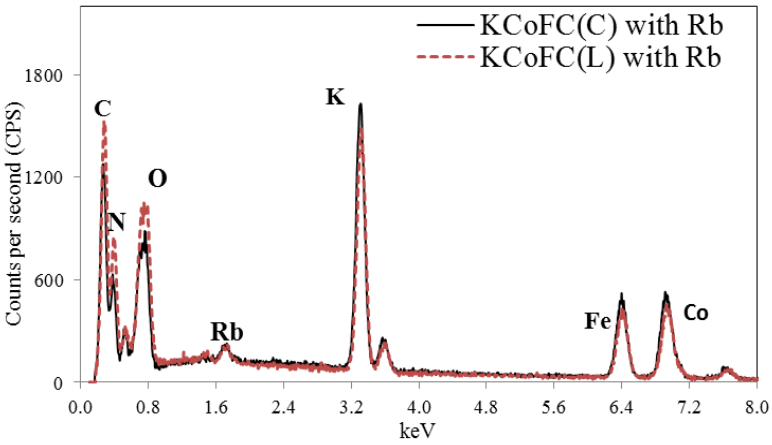

KCoFC(L) with Rb	% atomic ratio
K/Fe	1.0
Co/Fe	1.4

KCoFC(C) with Rb	% atomic ratio
K/Fe	0.97
Co/Fe	1.4

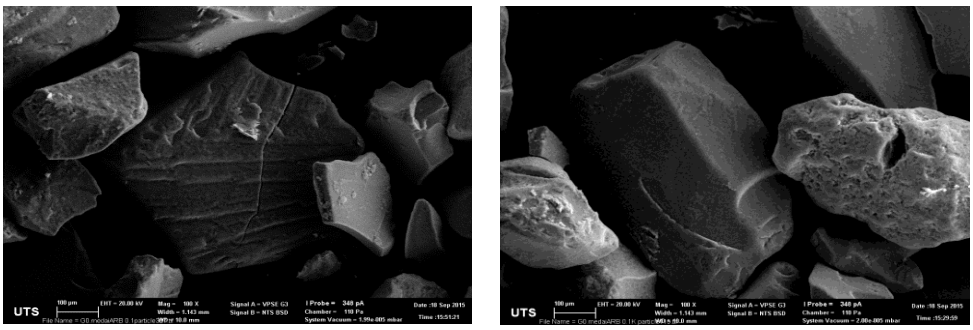

KCoFC(C) **KCoFC(L)**

Fig. 1. SEM-EDS analysis of KCoFC(C) and KCoFC(L) **(a)** original **(b)** after Rb sorption.

3.1.3. Powder X-ray diffraction (XRD) analysis

The XRD composition showed the same diffraction peaks for both the lab and commercial sorbent, confirming the similarity in crystal structure (**Fig. 2**). In this respect, previous studies on KCoFC sorbent, reported that main diffraction lines for KCoFC to be 2θ = 17.72, 25.24, 36.08, 40.56, 42.8, 52.2 and 58.64º [12, 25]. The corresponding sharp peaks were detected in this XDR analysis, verifying the positions of the main diffraction lines for both KCoFC(C) and KCoFC(L).

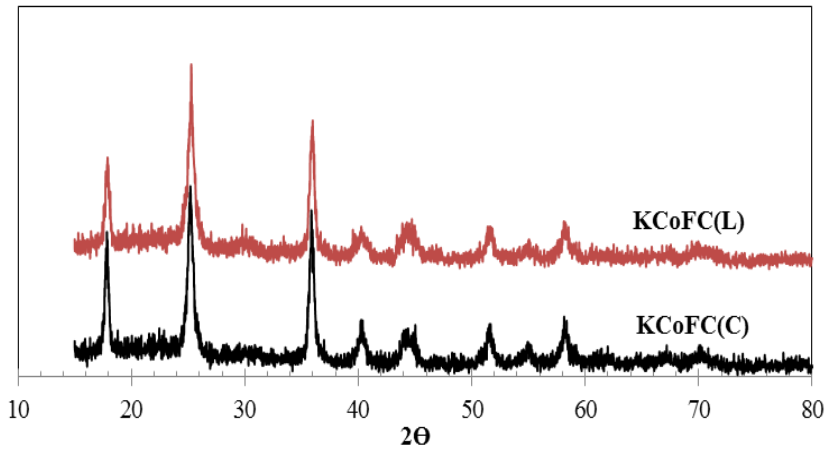

Fig. 2. XRD peaks of KCOFC(L) and KCoFC(C).

3.1.4. Surface area and pore volume

The surface area of KCoFC(L) was 55.4 m^2/g with a total pore volume of 0.26 cm^3/g while the average pore diameter was 18.8 nm. On the other hand, KCoFC(C) showed higher values for all these parameters (surface area 72.1 m^2/g, total pore volume 0.37 cm^3/g, pore diameter 20.5 nm) in comparison to KCoFC(L). This could be attributed to the difference in mixing and drying of the sorbent during commercial production. The respective average pore diameters of 18.8 and 20.5 nm for the two KCoFC indicate that these materials consist mainly of mesopores (2 – 50 nm).

3.2. Influence of pH on the sorption of Rb

The pH of the aqueous solution is an important controlling parameter in the sorption process because it influences the surface charge on the sorbent. To study the influence of pH, experiments were conducted between pH 3 to 10. Rb sorption capacity increased up to pH 7-8 and then declined as pH increased (**Fig. 3**). The maximum sorption capacity of Rb was achieved at a pH range of 7 to 8.

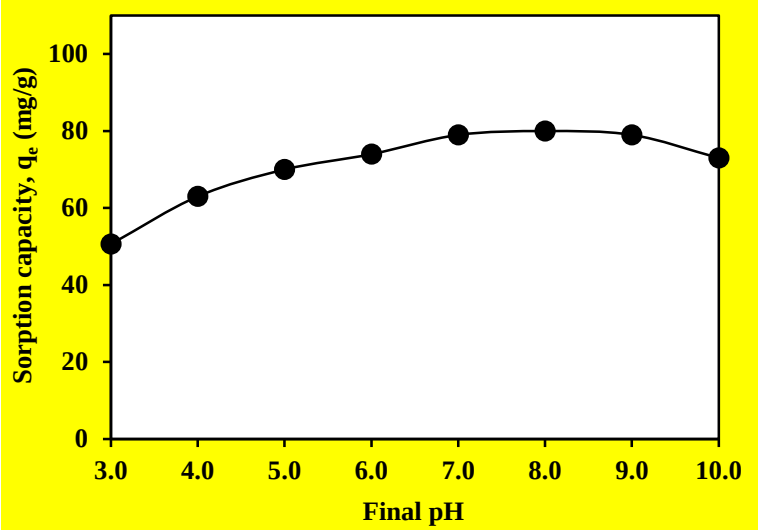

Fig. 3. Influence of pH on Rb sorption (C_o = 5 mg/L, KCoFC dosage = 0.05 mg/L).

The increased sorption was mainly due to an increase in the negative surface charge on the sorbent as indicated by the zeta potential trend (**Fig. 4**). Increased negative charge on the sorbent is expected to increase the sorption of positively charged ions such as Rb by electrostatic adsorption (outer sphere complexation). The lower Rb sorption at low pH is also due to the competition of H with Rb for sorption sites in the highly acidic solution where the concentration of H is high. At high pH (above 8), the presence of increased concentration of Na (arising from pH adjustment with NaOH) most likely competed with Rb sorption, thus reducing Rb sorption capacity. Since the maximum sorption capacity of Rb was obtained at a final pH range of 7 to 8, all further experiments were carried out at pH 7.0 ± 0.5.

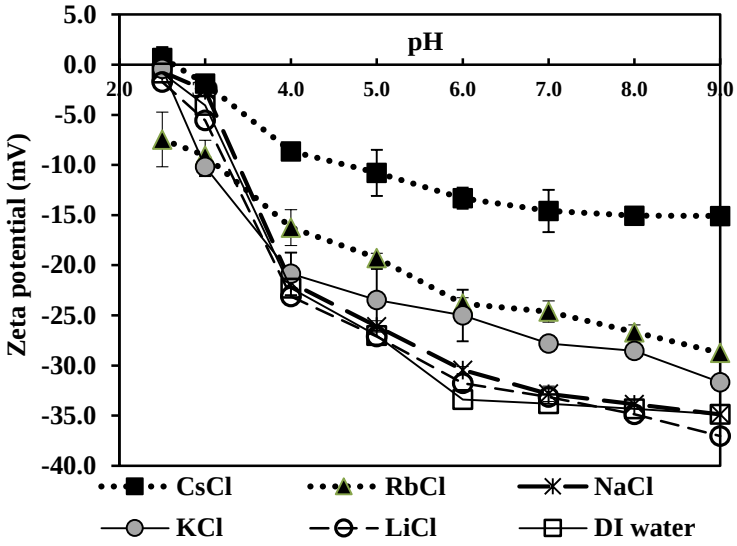

Fig. 4. Zeta potential trend as a function of pH for alkali metals (1 x10^{-4} M) and DI water (KCoFC dosage = 0.1 g/L).

Table 2. Hydrated and unhydrated ionic radius of alkali metals

Alkali metal	Hydrated ionic radius, Å [5]	Unhydrated ionic radius, Å [23]
Cs	2.26 - 2.28	1.68
Rb	2.28	1.48
K	2.32 - 3.31	1.33
Na	2.76 - 3.60	0.95
Li	3.40 - 4.70	0.60

3.3. Rb and Cs sorption capacity

Both KCoFC(L) and KCoFC(C) sorbents showed much higher sorption capacity for Rb and Cs than Li, Na and Ca at all equilibrium solution concentration of the metals (**Fig. 5**). As both KCoFC(C) and KCoFC(L) sorbents showed similar characteristics (SEM-EDX, chemical composition, XRD), a similar sorption capacity would be expected for both sorbents. However, a slightly higher sorption capacity was observed with KCoFC(C) compared to KCoFC(L). This could be attributed to the higher surface area and pore volume of the KCoFC(C).

The sorption data were modelled using Langmuir and Freundlich equations. The sorption data for Li, Na, and Ca did not satisfactorily fit to these models. However, the data for Rb and Cs fitted well to both the models with the fit being better for the Langmuir model (R^2 = 0.92 to 0.98) than for the Freundlich model (R^2 = 0.73 to 0.93) (**Fig. 5, Table 3**). Similar observations were reported by Petersková et al. [5] for Rb and Cs sorption on potassium hexacyanoferrate sorbent.

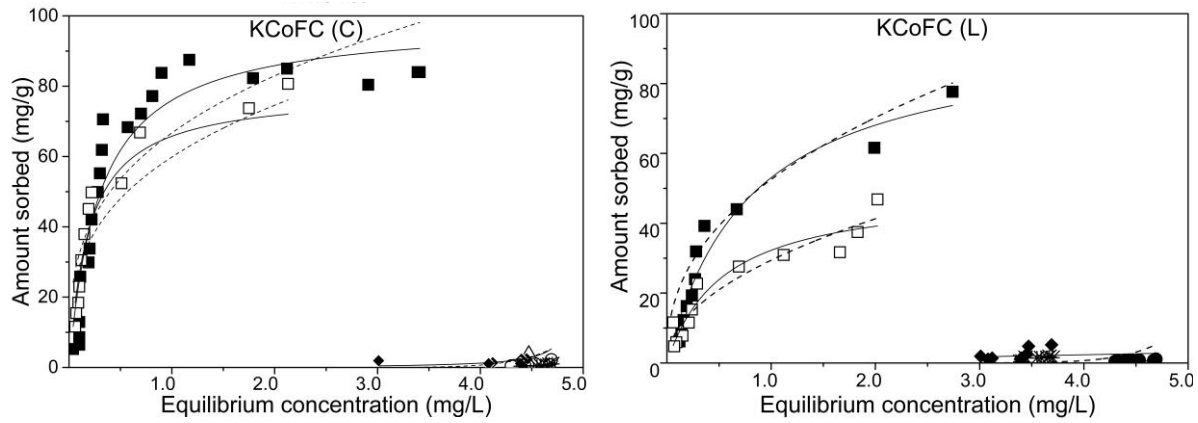

(a) **(b)**

Fig. 5. Sorption capacity of **(a)** KCoFC(C) **(b)** KCoFC(L) with Rb (■), Cs (□), Na(●), Li (◆) and Ca (✳) (── Langmuir model; ----- Freundlich model) (C_o of Rb and Cs = 5 mg/L, C_o of Ca, Na and Li = 20 mg/L, final pH 7 ± 0.5).

Table 3. Langmuir and Freundlich models parameters at final pH 7.0 ± 0.5.

Metal	Sorbent	Langmuir			Freundlich		
		Q_{max} (mg/g)	K_L (L/mg)	R^2	n	K_F (mg/g)(L/mg)$^{1/n}$	R^2
Rb	KCoFC(C)	100.1	3.7	0.98	1.7	71.4	0.86
	KCoFC(L)	96.2	1.2	0.95	1.8	48.2	0.86
Cs	KCoFC(C)	75.8	5.9	0.92	2.6	62.6	0.73
	KCoFC(L)	60.9	1.0	0.96	1.5	32.2	0.93

In the Langmuir model, the value of R_L as calculated from the formula, $R_L = 1/(1+C_m K_L)$ (where C_m is the maximum initial concentration of sorbate), indicates the favourability of the sorption process, such as unfavourable ($R_L > 1$), favourable ($0 < R_L < 1$) or irreversible (R_L

= 0) [20]. The calculated R_L values for Rb and Cs data were in the 0.04 to 0.25 range, indicating that the sorption process is favourable for both these metals.

Langmuir model fits to data showed that for Rb, a Q_{max} of 96.2 to 100.1 mg/g (1.13.to 1.17 mmole/g) was achieved for both the lab and commercial KCoFC. Comparatively, a lower Q_{max} was achieved for Cs at 60.9 to 75.8 mg/g (0.46 to 0.57 mmole/g) (**Table 3**). Previous studies on Rb and Cs sorption with commercial KCoFC (CsTreat) reported a similar pattern of relatively higher Rb sorption compared to Cs sorption [5,6,23]. For instance, Petersková et al. [5] reported a Q_{max} of 46.73 mg/g for Rb sorption and a Q_{max} of 32.36 mg/g for Cs sorption with a commercial KCoFC at pH 7.8 and equilibrium metal concentrations of 5-80 mg/L.

The capacity of alkali metal sorption on sorbents is generally in the order of Cs > Rb > K > Na > Li based on the hydrated radius of the ions (**Table 2**). The smaller the hydrated ionic radius, the closer the ion can reach the sorbent surface, and therefore the stronger the sorption. Based on the hydrated ionic radius, Cs should exhibit similar or higher sorption capacity compared to Rb. Conversely, a relatively higher sorption of Rb was observed in this study as well as in previous research. Lehto et al. [23] associated this phenomenon to the similar sizes of the KCoFC cavities within the lattice (1.47 Å) and the unhydrated Rb radius (1.48 Å) compared to the larger unhydrated Cs radius (1.61 Å). Therefore, Rb was able to achieve a higher penetration into the crystal lattices, displacing the K in the lattices, hence exhibiting a higher sorption capacity.

The occurrence of lattice ion exchange was evident as K was released with the sorption of Rb and Cs (**Table 4**). At equilibrium, the corresponding amount of K released was higher for Rb than for Cs, confirming the higher penetration of Rb into the KCoFC crystal lattice. Prout et al. [18] described this exchange reaction utilising the following equation:

$$K_2[CoFe(CN)_6] + 2\ Rb^+ \rightarrow Rb_2[CoFe(CN)_8] + 2\ K^+ \quad (8)$$

It is important to highlight that an additional amount of K release was detected (1.05-1.39 mmol/g) relative to the amount of Cs and Rb sorbed (**Table 4**). Previous studies related the excess fraction of K released to the dissolution of K from the sorbent in aqueous solution [23]. In line with this, the blank test with DI water showed 0.40 ± 0.19 mmol/g K release (**Table 4**). Upon subtracting the soluble K released from the total amount of K released when Rb and Cs were sorbed, the ratios of Rb and Cs sorbed to K released (mmoles) were 0.92 and 1.09, respectively. This indicates that there was stoichiometric electrochemical balance in the exchange process.

Table 4. Alkali metals sorption on KCoFC(L) and the corresponding amounts of K, Co and Fe released

Alkali metal	Equilibrium metal concentration (mg/L)	Metal sorbed (mmol/g)	K released (mmol/g)	Co released (mmol/g)	Fe released (mmol/g)
Rb	2.74	0.91 ± 0.11	1.39 ± 0.25	0.07 ± 0.05	0.05 ± 0.02
Cs	2.92	0.71 ± 0.09	1.05 ± 0.42	0.05 ± 0.02	0.04 ± 0.02
Na	4.81	0.14 ± 0.09	0.51 ± 0.38	0.06 ± 0.03	0.05 ± 0.01
Li	3.01	0.17 ± 0.08	0.58 ± 0.29	0.04 ± 0.02	0.05 ± 0.02
DI (blank)		--	0.40 ± 0.19	0.02 ± 0.03	0.03 ± 0.01

During the Rb and Cs sorption process very little Co and Fe were released, which indicated that Rb and Cs were not exchanging with Co and Fe in the crystal lattice (**Table 4**). This is because Co and Fe are transitional metal cations bridged through cyano (CN) groups in the lattice structure which cannot be exchanged with the alkali metals Rb and Cs [26]. Loos-

Neskovic et al. [26] reported that the cyano groups bridged to Fe and Cu in $K_2[CuFe(CN)_6]$ provided negative charges which were balanced by the positively charged K in the body centre of the lattice.

3.3.1. KCoFC sorption capacity with other alkali metals

While Rb and Cs exhibited high sorption capacity on KCoFC, other metals such as Li, Na and Ca remained mostly unchanged in the initial solutions without having any appreciable sorption (**Fig. 5**). The difference in the sorptivity between the metals can be explained on the basis of the relative size of the target ions and the pores or cavities of the sorbent as presented in **Table 2**. The amounts of Na and Li sorbed were much lower than those of Rb and Cs because of their lower degree of ion exchange with lattice K as seen from the smaller amounts of K released when they were sorbed (**Table 4**). This lower degree of ion exchange is due to the smaller unhydrated ionic radius of Na and Li (**Table 2**). Most of the K released during the sorption of Li and Na was due to the release of water soluble K in the sorbent. Another reason for the lower sorption of Li and Na than Rb and Cs is that these metals were more strongly hydrated and therefore bind more weakly to the KCoFC surface (**Table 2**). The zeta potential data on KCoFC supports this surface sorption difference between the metals. The negative zeta potential in the presence of monovalent metals increased in the order of the degree of ion hydration (Li > Na > K > Rb > Cs) (**Fig. 4**). The less hydrated monovalent cations (Rb, Cs) bind more strongly to the KCoFC surface resulting in relatively lower negativity of the zeta potential (-12 to -23 compared to -27 to -33 for Li, Na, K at pH 7).

3.4. Rb sorption kinetics

Kinetics of sorption governs the uptake rate of sorbates and is therefore an important aspect in assessing the sorbent's characteristics. The kinetic results of KCoFC(L) displayed an

increased sorption capacity of Rb with contact time (**Fig. 6)**. A maximum sorption of around 63% was achieved within 15 h. In correspondence with the sorption of Rb, K release was detected over the entire duration of sorption (**Fig. 6**). The number of mmoles of K released at any time was equivalent to the number of moles of Rb sorbed (additional K released from sorbent dissociation in aqueous solution was offset by the blank DI correction as presented in **Table 4)**. The majority of K released occurred when Rb exchanged with K inside the KCoFC lattice.

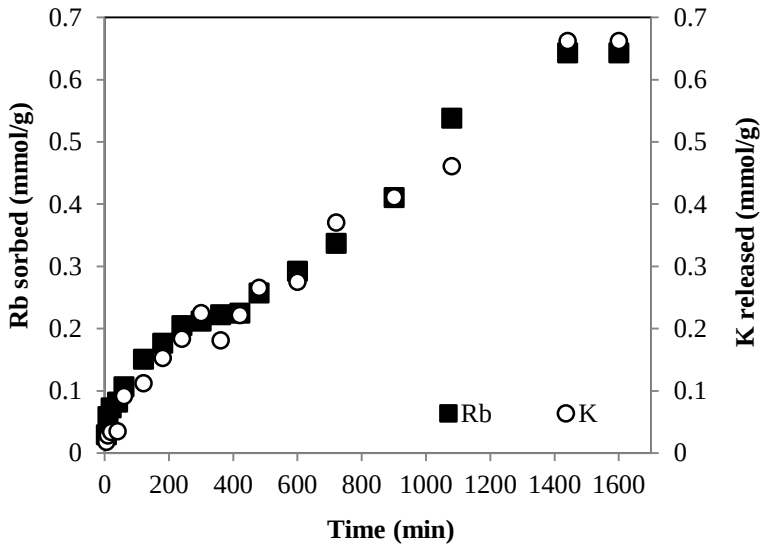

Fig. 6. Rb sorbed and K released as a function of time (C_o = 5 mg/L, KCoFC dosage = 0.05 g/L, pH 7).

The sorption kinetics data was analysed using different kinetic models. The results showed that the data fitted slightly better to PSO model than to PFO model with R^2 values of 0.97 and 0.92, respectively (**Fig. 7**). Furthermore, for the PFO model, the q_e value of 63.4 mg/g derived from the model differed from the experimental q_e value of 56.6 mg/g. On the other hand, for the PSO model, the q_e value of 55.5 mg/g derived from the model agreed better with the experimental value. Therefore the kinetics data is better described by the PSO model. Better

description of the data by PSO suggested that the sorption of Rb is mainly controlled by chemical process [20] which depends on the concentration of Rb in solution and the number of sorption sites on KCoFC that were unoccupied by Rb.

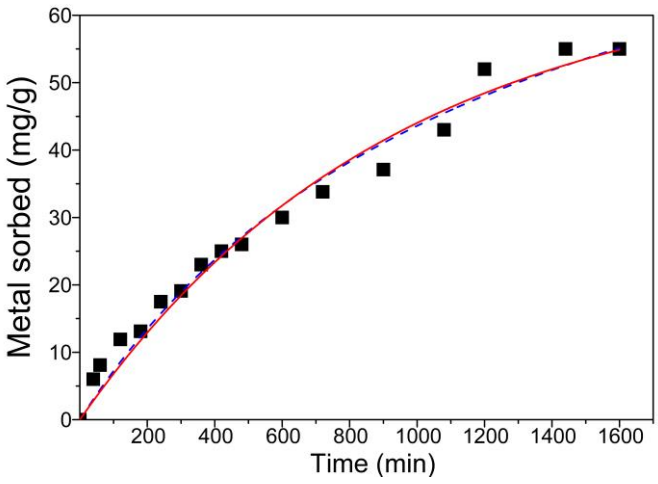

Fig.7. Kinetic model fit for experimental data of Rb sorption on KCoFC(L) (Rb experimental data (■), ── PFO; -----PSO) (C_o = 5 mg/L, KCoFC dose 0.05 g/L, pH 7).

.

Generally, kinetic models describe the whole sorption process but the actual rate limiting steps are not provided in detail. The transportation of Rb from the bulk solution to the KCoFC surface can be described by: (1) bulk diffusion from the external solution to the film surrounding the KCoFC particle (bulk diffusion) (2) diffusion of Rb through the film surrounding the KCoFC particles (film diffusion); (3) diffusion of Rb through the hydrated pores of the KCoFC particle (intraparticle diffusion); and (4) chemical exchange reaction of Rb at the internal particle surface and exchange with structural K (chemical reaction). Bulk diffusion is negligible in determining the limiting rate because of enough agitation in batch experiments which does not allow any concentration gradients to build-up. Intraparticle diffusion is highly likely because the particles are mesoporous. In this study, the Weber and Morris intraparticle diffusion model was used to represent the intraparticle diffusion trend with

time for KCoFC [20,21]. According to Weber and Morris [21], if intraparticle diffusion is the rate limiting step in the sorption process, the plot of q_t versus $t^{0.5}$ would be a straight line that passes through the origin. In this study, the experimental data showed two linear portions (**Fig. 8**). The first linear portion from 5 min up to 4 h can be attributed to the transport by intraparticle diffusion of Rb through the pores and channels This is followed by a slow step where Rb exchanged with the structural K that is located in the body/centre of the cubic caged KCoFC [Table 4, Fig. 6] and the reduced rate of intraparticle diffusion resulting from the low Rb concentration in solution [27]. As the entire plot was not linear and did not pass through the origin, film diffusion, intra-particle diffusion, and exchange with structural K appeared to have occurred simultaneously during the sorption process. However, as film diffusion is faster than intraparticle diffusion, it would have been mostly completed within the first 5 min before most of the intraparticle diffusion operated. Intraparticle diffusion and exchange of Rb with structural K appear to be the major rate controlling steps.

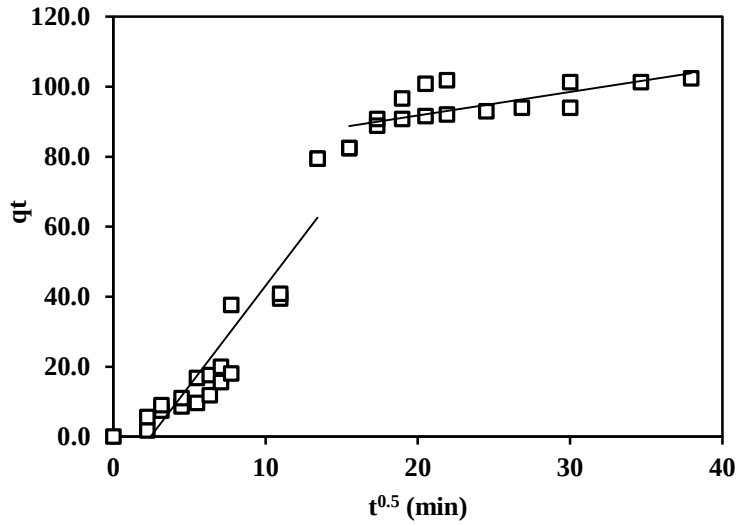

Fig. 8. Intraparticle diffusion kinetics of Rb (C_o = 5 mg/L, KCoFC dose 0.05 g/L, pH 7).

The results of the kinetic study clearly demonstrated that Rb was first adsorbed on to the surface of the KCoFC prior to the K ion exchange reaction within the crystal lattice as

indicated by previous studies [23,28]. In line with this, as shown in the zeta potential trend **(Fig. 4)**, the negativity of the surface potential/charge of KCoFC declined in the presence of Rb, verifying the strong surface sorption of Rb. At the same time, K was released over time when Rb was sorbed as shown in **Fig. 6**, confirming that ion exchange occurred between Rb in solution and K in the sorbent lattice.

3.5. Effect of competing ions on Rb sorption

An important factor that influences the performance of a sorbent for a target metal is the selective sorption of the metal in the presence of competitor ions. In order to verify the selectivity of KCoFC(L) for Rb, the sorption capacity of Rb was evaluated in the presence of other competitor monovalent alkali metals (Cs, Li, Na, K) as well as the divalent metal, Ca at a range of concentrations (**Fig. 9**). All experiments were conducted with an initial Rb concentration of 5 mg/L and sorbent dosage of 0.05 g/L while the competitor ions concentration increased from 5 to 20 mg/L.

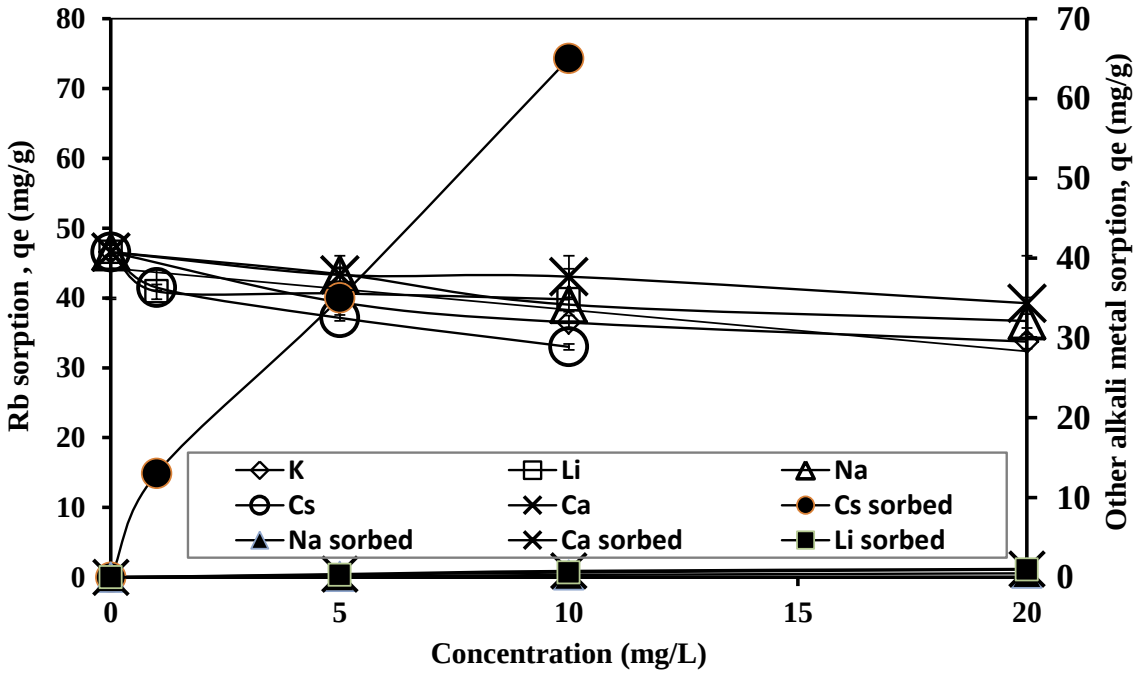

Fig. 9. Effect of coexisting alkali metals and Ca on Rb sorption on KCoFC(L) (KCoFC dose 0.05 g/L, initial Rb concentration 5 mg/L, pH 7).

The results showed that when Rb and Cs were present together at the same concentration (5 mg/L), the individual Rb and Cs sorption capacities of 49.9 mg/g and 40.1 mg/g, decreased slightly by 7-12%. This indicated that KCoFC has a high selectivity for both Cs and Rb, and therefore was only slightly affected by each other's co-ion effect. Naturally, at higher Cs concentration (10 mg/L), the Rb sorption reduced further by 25-29%. However, in many situations such as in seawater, the Cs concentration (0.0005 mg/L) is much lower than Rb concentration (0.12 mg/L) and therefore Cs is not expected to affect the sorption of Rb by KCoFC [6].

Comparatively, Rb sorption was minimally affected by the presence of alkali metals, Li, Na, and K and divalent alkaline earth metal, Ca at concentrations of 5 to 20 mg/L (**Fig. 9**). At a concentration of 20 mg/L of the other metals, the Rb sorption capacity was reduced only

by 10-15% and the sorption of Li, Na, K, and Ca was less than 2 mg/g. Therefore, Rb sorption on KCoFC was only influenced by the presence of Cs at a higher concentration while the influence of other metals (Li, Na, K, Ca) was minimal.

3.6. Rb desorption capacity

At a concentration of 0.1 M of desorption agent, the percentage of Rb desorption declined in the order of KCl (74.0%), KOH (47.3%), NaOH (46.5%), NaCl (10.5%), HCl (1.75%), and HNO_3 (0.75%) (**Fig. 10**). Percentage desorption with H_2O was the lowest (0.4%). Desorbing agent with K was more efficient than with Na in desorbing Rb because of the closer unhydrated ionic radius of K and Rb than Na and Rb (**Table 2**), thus K was able to effectively exchange with sorbed Rb inside the KCoFC lattice. At a higher concentration of KCl (1.0 M), 98-100% of Rb desorption from KCoFC was achieved.

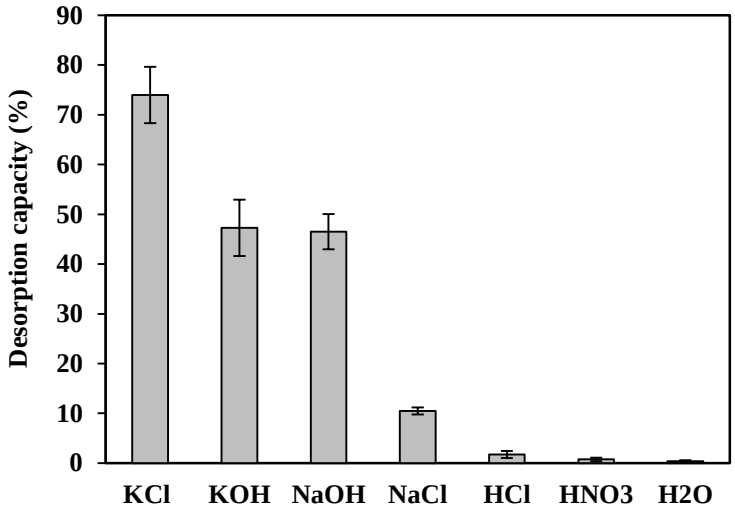

Fig. 10. Rb desorption with 0.1 M desorbing reagents (after sorption at C_o = 5 mg/L, KCoFC dose 0.1 g/L).

4. Conclusions

The affinity of KCoFC sorbent for Rb was evaluated using a laboratory prepared KCoFC (KCoFC(L)). Detailed characterisation (chemical composition, SEM-EDX and XRD) of KCoFC(L) established its similarity to the commercial KCoFC. The major findings for the Rb sorption characteristics of KCoFC(L) are as follows:

- Rb sorption increased from pH 3 to 7 and remained the same at pH 7 to 8, in accordance with the increase of zeta potential negativity.
- Sorption capacity of alkali metals and alkaline earth metal Ca on KCoFC followed the decreasing order Rb > Cs > Li, Na, Ca. The higher sorption capacity of Rb compared to the other metals had two explanations. Firstly, it is due to greater surface sorption on the KCoFC as a result of its lower hydrated ionic radii. This was supported by the observation that the negative zeta potential of KCoFC was lower for Rb than for Li, Na and Ca. Secondly, Rb made a greater penetration into the crystal lattice to replace structural K in the body centre of KCoFC than other metals including Cs. Rb released

the largest amount of K, followed by Cs due to Rb and K sharing similar unhydrated ionic radius. Sorption data for Rb and Cs at pH 7.0 ± 0.5 satisfactorily fitted to the Langmuir sorption model. A higher Langmuir maximum sorption capacity of 96.2 mg/g was achieved with Rb compared to 60.6 mg/g for Cs.

- The Rb sorption kinetics data fitted satisfactorily to PSO model with intraparticle diffusion and exchange of Rb with structural K acting as major rate limiting steps.
- The presence of co-existing elements such as Li, Na and Ca only minimally influenced Rb sorption, thereby indicating the selective sorption of KCoFC for Rb. Only at higher concentrations did Cs reduce the Rb sorption capacity.
- A high desorption capacity (78- 80%) of Rb was able to be achieved with 0.1 M KCl. Up to 100% desorption was possible with 1.0 M KCl.

Acknowledgements

This work was funded by Australian Research Council Discovery Research Grant (DP150101377). We thank Mr. Phillip Thomas in Adelaide, South Australia for proof-reading/editing this paper.

References

[1] Ghosh, S., Bhagwat, A.R., Renshaw, C.K., Goh, S., Gaeta, A.L., Kirby, B.J., Low-light-level optical interactions with rubidium vapor in a photonic band-gap fiber. Phys. Rev. Lett. 97 (2006) 023603.

[2] Jandova, J., Dvořák, P., Formánek, J., Vu, H.N., Recovery of rubidium and potassium alums from lithium-bearing minerals. Hydrometallurgy 119 (2012) 73-76.

[3] Hétet, G., Hosseini, M., Sparkes, B., Oblak, D., Lam, P.K., Buchler, B.C., Photon echoes generated by reversing magnetic field gradients in a rubidium vapor. Opt. Lett. 33 (2008) 2323-2325.

[4] Hosseini, M., Sparkes, B.M., Campbell, G., Lam, P.K., Buchler, B.C., High efficiency coherent optical memory with warm rubidium vapour. Nat. Commun. 2 (2011) 1-5.

[5] Petersková, M., Valderrama, C., Gibert, O., Cortina, J.L., Extraction of valuable metal ions (Cs, Rb, Li, U) from reverse osmosis concentrate using selective sorbents. Desalination 286 (2012) 316-323.

[6] Jeppesen, T., Shu, L., Keir, G., Jegatheesan, V., Metal recovery from reverse osmosis concentrate. J. Clean. Prod. 17 (2009) 703-707.

[7] Le Dirach, J., Nisan, S., Poletiko, C., Extraction of strategic materials from the concentrated brine rejected by integrated nuclear desalination systems. Desalination 182 (2005) 449-460.

[8] Ye, X., Wu, Z., Li, W., Liu, H., Li, Q., Qing, B., Guo, M., Ge, F., Rubidium and cesium ion adsorption by an ammonium molybdophosphate–calcium alginate composite adsorbent. Colloids Surf., A. 342 (2009) 76-83.

[9] Mohite, B., Burungale, S., Separation of rubidium from associated elements by solvent extraction with dibenzo-24-crown-8, Anal. Lett. 32 (1999) 173-183.

[10] Shamsipur, M., Alizadeh, K., Hosseini, M., Mousavi, M.F., Ganjali, M.R., PVC Membrane and Coated Graphite Potentiometric Sensors Based on Dibenzo-21-Crown-7 for Selective Determination of Rubidium Ions. Anal. Lett. 38 (2005) 573-588.

[11] Yang, H., Sun, L., Zhai, J., Li, H., Zhao, Y., Yu, H., In situ controllable synthesis of magnetic Prussian blue/graphene oxide nanocomposites for removal of radioactive cesium in water. J. Mater. Chem. A. 2 (2014) 326-332.

[12] Moon, J., Lee, E., Kim, H., Ion exchange of Cs ion in acid solution with potassium cobalt hexacyanoferrate. Korean J. Chem. Eng. 21 (2004) 1026-1031.

[13] El-Kamash, A., Evaluation of zeolite A for the sorptive removal of Cs^{+} and Sr^{2+} ions from aqueous solutions using batch and fixed bed column operations. J. Hazard. Mater. 151 (2008) 432-445.

[14] Saberi, R., Nilchi, A., Garmarodi, S.R., Zarghami, R., Adsorption characteristic of 137Cs from aqueous solution using PAN-based sodium titanosilicate composite. J. Radioanal. Nucl. Chem. 284 (2010) 461-469.

[15] Park, Y., Lee, Y., Shin, W.S., Choi, S., Removal of cobalt, strontium and cesium from radioactive laundry wastewater by ammonium molybdophosphate–polyacrylonitrile (AMP–PAN). Chem. Eng. J. 162 (2010) 685-695.

[16] Gibert, O., Valderrama, C., Peterkóva, M., Cortina, J.L., Evaluation of selective sorbents for the extraction of valuable metal ions (Cs, Rb, Li, U) from reverse osmosis rejected brine. Solvent Extr. Ion Exch. 28 (2010) 543-562.

[17] Tusa, E., Harjula, R., Lehto, J., Use of highly selective ion exchangers for minimization of waste volumes. Proceedings of Waste Management Symposium, Tucson, Arizona, USA, (2001).

[18] Prout, W., Russell, E., Groh, H., Ion exchange absorption of cesium by potassium hexacyanocobalt (II) ferrate (II). J. Inorg. Nucl. Chem. 27 (1965) 473-479.

[19] Nilchi, A., Malek, B., Maragheh, M.G., Khanchi, A., Investigation of the resistance of the potassium copper nickel hexacyanoferrate (II) ion exchanger against gamma irradiation. Radiat. Phys. Chem. 68 (2003) 837-842.

[20] Rusmin, R., Sarkar, B., Liu, Y., McClure, S., Naidu, R., Structural evolution of chitosan–palygorskite composites and removal of aqueous lead by composite beads. Appl. Surf. Sci. 353 (2015) 363-375.

[21] Weber, W., Morris, J., Intraparticle diffusion during the sorption of surfactants onto activated carbon. J Sanit. Eng. Div. Am. Soc. Civ. Eng. 89 (1963) 53-61.

[22] Mardan, A., Ajaz, R., Mehmood, A., Raza, S., Ghaffar, A., Preparation of silica potassium cobalt hexacyanoferrate composite ion exchanger and its uptake behavior for cesium. Sep. Purif. Technol. 16 (1999) 147-158.

[23] Lehto, J., Paajanen, R., Harjula, R., Selectivity of potassium cobalt hexacyanoferrate (II) for alkali and alkaline earth metal ions. J. Radioanal. Nucl. Chem.164 (1992) 39-46.

[24] Vincent, C., Hertz, A., Vincent, T., Barré, Y., Guibal, E., Immobilization of inorganic ion-exchanger into biopolymer foams–Application to cesium sorption. Chem. Eng. J. 236 (2014) 202-211.

[25] Nilchi, A., Khanchi, A., Atashi, H., Bagheri, A., Nematollahi, L., The application and properties of composite sorbents of inorganic ion exchangers and polyacrylonitrile binding matrix. J. Hazard. Mater. 137 (2006) 1271-1276.

[26] Loos-Neskovic, C., Ayrault, S., Badillo, V., Jimenez, B., Garnier, E., Fedoroff, M., Jones, D., Merinov, B., Structure of copper-potassium hexacyanoferrate (II) and sorption mechanisms of cesium. J. Solid State Chem. 177 (2004) 1817-1828.

[27] Yue, Q., Li, Q., Gao, B., Wang, Y., Kinetics of adsorption of disperse dyes by polyepicholorohydrin-dimethylanine cationic polymer/bentonite. Sep. Purif. Technol. 54 (2007) 279-290.

[28] Lee, E.F., Streat, M., Sorption of caesium by complex hexacyanoferrates iv. ion exchange kinetics and mechanism of sorption by potassium copper ferrocyanide. J. Chem. Technol. Biotechnol. 33 (1983) 87-96.